Science of Sintering, **55** (2023)145-158

https://doi.org/10.2298/SOS220429002P

UDK: 692.533.1; 622.785; 669.14; 553.532

Novel Basalt-Stainless Steel Composite Materials with Improved Fracture Toughness

Vladimir Pavkov[1*)], Gordana Bakić[2], Vesna Maksimović[1], Ivana Cvijović-Alagić[1], Dušan Bučevac[1], Branko Matović[1]

[1]Department of Materials Science, Vinča Institute of Nuclear Sciences - National Institute of the Republic of Serbia, University of Belgrade, Mike Petrovića Alasa 12-14, 11000 Belgrade, Serbia

[2]Faculty of Mechanical Engineering, University of Belgrade, Kraljice Marije 16, 11000 Belgrade, Serbia

Abstract:

This paper presents the technological process for obtaining basalt-stainless steel composite materials and testing their physical and mechanical properties. The phases of the technological process consist of: milling, homogenization, pressing, and sintering to obtain composite materials with improved fracture toughness. Andesite basalt from the deposit site "Donje Jarinje", Serbia, was used as a matrix in the composites, while commercial austenitic stainless steel 316L in the amount of 0-30 wt.% was used as a reinforcement. Although the increase of 316L amount caused a continuous decrease in the relative density of sintered samples, the relative density of sample containing 30 wt.% of 316L was above 94%. The 316L grains, which possess a larger coefficient of thermal expansion than the basalt matrix, shrinking faster during cooling from sintering temperature resulting in the formation of compressive residual stress in the basalt matrix surrounding the spherical steel grains. The presence of this stress activated toughening mechanisms such as crack deflection and toughening due to compressive residual stress. The addition of 20 wt.% of reinforcing 316L particles increased the fracture toughness of basalt by more than 30%. The relative density of these samples was measured to be 97%, whereas macrohardness was found to be 6.2 GPa.

Keywords*: Composite materials; Andesite basalt; Stainless steel 316L; Sintering; Cracks.*

1. Introduction

The wide use of ceramic materials is based on a good combination of properties, such as relatively low density, excellent resistance to high temperatures, high hardness, good wear-resistance, and chemical inertness [1,2]. The main disadvantage, which still prevents the wider application of ceramics, is the tendency towards brittle fracture. The brittle fracture represents the separation of atomic levels. Each grain has a separate plane suitable for separating atomic planes, which causes a fracture plane. Cracks in brittle materials such as ceramics are not stable and spread rapidly without increasing stress, due to small plastic deformation. The crack often spreads by splitting-breaking atomic bonds along specific crystallographic planes [3,4].

*) **Corresponding author:** pavkow@vin.bg.ac.rs

The lack of plastic deformations results in the formation of microcracks that are not visible to the naked eye but cause a sudden fracture. Once cracks are formed, the mechanical properties and structure of ceramic materials systematically degrade irreversibly, leading to catastrophic fracture, and compromising the safety of material users. Sudden, catastrophic failure is the most posted damage mechanism in technical ceramics caused by the rapid growth of a single crack. The growth rate of crack is so high that crack arrest is almost impossible [5-8]. A brittle fracture can progress at speeds of up to 1600 m/s, while a ductile fracture progresses at speeds of about 500 m/s, although it can be slower [9]. For this reason, high brittleness and insignificant ductility impede the wider use of ceramics as advanced technical materials [10].

The fracture toughness of ceramic materials is still low, compared to metallic materials, and for this reason, novel composite materials are developed daily to increase the fracture toughness of the ceramic matrix. Many technical solutions require the application of novel materials, which require properties that do not have pure metal material or its alloys as well as ceramic materials. Such materials are called composite materials. Composite materials have applications in various industries due to their advanced properties [11].

The division of composite materials based on the type of matrix can be Metal Matrix Composites (MMC), Polymer Matrix Composites (PMC), and Ceramic Matrix Composites (CMC) [3]. One of the key tasks in developing composite materials with a ceramic matrix is to resist the sudden spread of cracks, *i.e.* increasing fracture toughness. The term initial crack is attached to the ceramic matrix, while crack propagation is prevented by reinforcements, which may be in the form of particles, fibers, or laminates.

Today, environmentally friendly and lightweight materials with good mechanical properties produced from low-cost raw materials are highly required. The material that meets all of these criteria is basalt. Basalt is a natural igneous rock of volcanic origin. It covers about 70% of the Earth's crust [12]. Basalt belongs to the group of grey-to-black colored and extremely hard rocks. Basalt rock processing technology is completely eco-friendly, which is very important for the ecology, energy- efficiency as well as economy of the modern age. Due to its good properties, such as low thermal conductivity, high oxidation resistance, high softening and melting temperatures [13], high chemical durability, high resistance to abrasion and corrosion [14-16], high strength and hardness [17], low viscosity [18], minimal moisture absorption, ability to withstand high temperatures, sound absorption properties [19, 20], exceptional compressive strength resulted in the use of basalt-based products in various industrial applications from civil and mechanical engineering, agriculture, construction industry, and mining, to the transportation industry, metallurgy [21-26], and as a decorative material [25, 27]. Basalt products do not show toxic, carcinogenic, mutagenic, or teratogenic effects [28], therefore it can be said that basalt is non-hazardous material [29]. Also, basalt, as well as sphene based glass-ceramic [30], is an excellent material for storing nuclear waste. Today, basalt powder can be used as reinforcement in the polymer matrix to obtain novel hybrid composite materials with improved cavitation resistance [31]. However, basalt, and other ceramic materials, has a brittle fracture and low fracture toughness which in most cases limits their application in various industries.

In the development of civilization, the significance of steel is reflected in the fact that the average annual quantity of steel produced in the World is about ten times bigger than the total amount produced of all other metals and alloys. Commercial stainless steels have a significant application in making machine elements and constructions in the industry because of their outstanding properties. The main properties of austenitic stainless steels are non-magneticity, high plasticity, high toughness, high strength-to-mass ratio, and good low-temperature properties, such as oxidation and corrosion resistance. A material such as austenitic stainless steel 316L has found wide application in the chemical and petrochemical industries [32,33], the nuclear industry [34], the pharmaceutical industry [35], the manufacture of medical implants [36,37], biomedicine [38], aerospace, agriculture,

construction [39] as well as at water desalination plants due to their excellent resistance to seawater [40]. Metallic materials such as austenitic stainless steel have higher ductility, which allows them to decompose stress concentrations by plastic deformation and thus stop the sudden propagation of the crack. Therefore, they can absorb more energy under impact load, because they deform plastically before breaking.

Although basalt shows numerous advantages for application in various industrial areas, it has a brittle fracture and low fracture toughness as other ceramic materials. For this reason, the presented research aimed to define the optimal technological process for obtaining composite materials based on basalt as matrix and stainless steel as reinforcement with increased fracture toughness relative to the monolithic basalt. As far as the authors know, this is the first time that basalt-stainless steel composite materials have been obtained by sintering using starting powder of basalt and powder of stainless steel.

2. Materials and Experimental Procedures

2.1 Materials and Synthesis

Basalt

As a starting material for the matrix of composite materials, the crushed basalt aggregate 1 to 5 mm in size (Fig. 1), supplied from the deposit site "Donje Jarinje", Serbia, was used. Basalt from this deposit site is noticeably black colored and classified as the andesite basalt [26,28]. It can also be found in the literature under the name the basaltic andesite [41].

Fig. 1.

Fig. 1. The crushed andesite basalt aggregate.

Stainless steel

In this experiment, as the reinforcement of composite materials, was used austenitic stainless steel. A starting powder of austenitic stainless steel diameter from 45 to 90 μm was used. Smaller particles were not at our disposal. According to chemical composition and physical properties, the powder of austenitic stainless steel corresponds to commercial grade steel SURFIT TM 316L [42,43]. In the following text, the austenitic stainless steel will be designated as 316L.

The 316L powder has a spherical shape which is obtained by gas atomization, Fig 2. The particles have satellites formed during the cooling of the droplets in the atomization process, which can be clearly seen in Fig. 2. During the disintegration of the liquid jet by gas,

the smaller droplets solidified faster and came into contact with the partially solidified larger droplets.

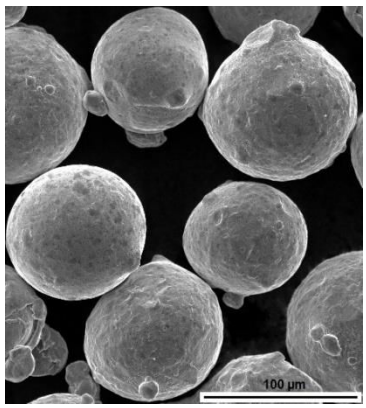

Fig. 2. SEM of 316L gas atomized stainless steel powder.

To obtain the powder, the andesite basalt aggregate was milled in a tungsten-carbide vibrating cup mill Fritsch Pulverisette 9, Germany. The milling lasted 60 min in a dry state at 800 rpm. The laser particle size analyzer Mastersizer 2000, Malvern Instruments Ltd., UK, was used to determine the particle size distribution. After milling, the particle size distribution of the andesite basalt powder was d(0.1)= 0.440 µm, d(0.5)= 1.463 µm, and d(0.9)= 6.844 µm, Fig 3.

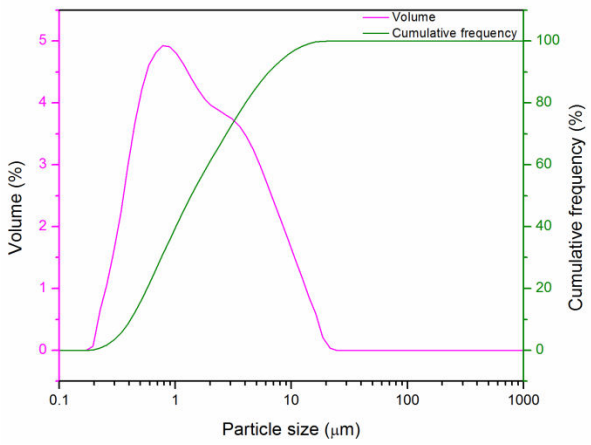

Fig. 3. Particle size distribution of the andesite basalt powder after 60 min dry milling.

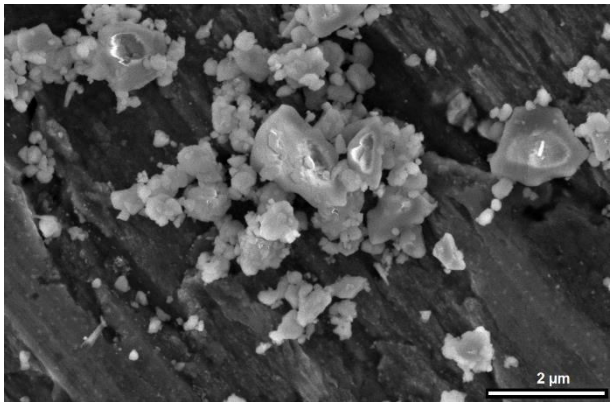

Fig. 4. SEM micrograph of the fine andesite basalt powder after 60 min dry milling.

The morphology of the andesite basalt powder obtained by milling is shown in Fig. 4. Clearly is visible the presence of angularly shaped particles with a rough surface on the SEM micrograph as well as the agglomeration of small powder particles.
Fig. 4.

The obtained fine powder of andesite basalt was mixed with 0.6 wt.% of commercial paraffin wax binder. Mixing lasted 10 min in a ceramic mortar by hand.

Thereafter, powder of 316L was added to the ceramic mortar in an amount of 5, 10, 15, 20, 25, and 30 wt.%, and then the whole mixture (powder of andesite basalt, 316L and binder) was mixed for another 20 min by hand. The spherical particles of 316L powder are suitable because they exhibit low interparticle friction, and high mobility during mixing [44]. For this reason, it takes less time to homogenize the powders during mixing which is advantageous from the aspect of composite material production.

After homogenization, the powders mixture is preloaded under a cold uniaxial and one-sided pressure of 50 MPa to obtain cylindrical green compacts 12 mm in diameter. After that, green compacts were cold isostatic pressed (CIP) under a pressure of 230 MPa for 2 min to increase their density.

To remove the binder and organic impurities, moisture, chemically bonded water from andesite basalt, the green compacts first, were slowly heated up in the air to 100°C at the heating rate of 1 °C/min and held at this temperature for 60 min. Then, additionally heated up at the same rate to 650°C and held for 60 min. After that, the green compacts were heated to the sintering temperature at the heating rate of 5 °C/min. Sintering was performed at 1060 °C for 60 min. The cooling rate to room temperature was 5 °C/min. The green compacts were sintered in the air in the laboratory high-temperature electric resistance box furnace Elektron VTP-03, Serbia. With these parameters, the highest relative density of sintered andesite basalt was obtained, which in this case represents the matrix of the composites.

2.2 Materials characterization

The pycnometric densities of andesite basalt powder and 316L powder were obtained using a pycnometer, distilled water, and analytical balance KERN ADB 100-4, Germany, with an accuracy of ± 0.001 g. Archimedes' method was used for the measurement relative density of the sintered composite samples.

To examine the microstructural characteristics of the sintered composite samples these samples were ceramographic prepared. The ceramographic preparation method involved grinding with SiC abrasive paper 1000 grit and polishing with 1 μm diamond paste. The microstructure of sintered composite materials was investigated by a light optical microscope (LOM) Zeiss Axioplan LM, Zeiss, Germany. Morphological characterization of the andesite basalt powder and 316L powder was performed using an SEM Tescan VEGA TS 5130 MM, Tescan, Czech Republic.

The macrohardness and fracture toughness of the sintered composite samples were determined utilizing the Vickers indentation hardness tester. All Vickers hardness and fracture toughness measurements were conducted at 5 measuring points of each sample. Applying a load of 3 kgf (29.421 N) was used to determine the macrohardness and the fracture toughness of the composite samples by model Buehler Identamet 1114, Buehler, Germany. The Vickers macrohardness (HV_3 [GPa]) was calculated [45,46] and measured in the andesite basalt matrix, in the zone around the 316L grains. The applied load of 3 kgf was used to form longer cracks in the composite matrix and to monitor their propagation when encountering the reinforcement. According to Eq. (1), the half-penny crack model was used for calculating fracture toughness in brittle materials [46,47]:

(1)

$$K_{IC} = 0.0752 \cdot \frac{P}{c^{\frac{3}{2}}}$$

where K_{IC} is the fracture toughness [MPa√m], P is the indentation load [N], while c is the measured crack length [m]. If a [m] is the half-diameter of the indented section and c/$a \geq 2$ then the crack model can be considered as the half-penny model.

3. Results and Discussion

3.1. Relative density

The measured pycnometric densities of andesite basalt powder and 316L powder were 2630 kg/m^3 and 7930 kg/m^3, respectively which is in a good agreement with the literature data [28,48]. These values are used to calculate the relative density of sintered composite samples assuming the mixture rule. The effect of the 316L amount on the relative density of sintered composite samples is shown in Fig. 5.

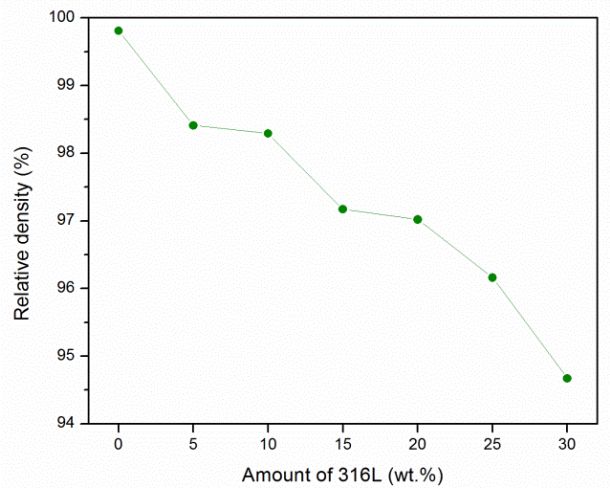

Fig. 5. Effect of 316L amount on relative density of the composite samples sintered at 1060°C for 60 min.

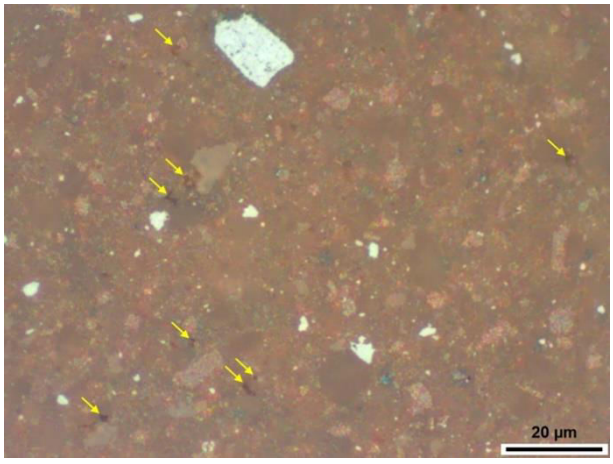

Fig. 6. LOM micrograph of polished surface of the monolithic andesite basalt sintered at 1060°C for 60 min.

The highest relative density of 99.81% was measured in monolithic basalt, *i.e.* pure andesite basalt without 316L particles. The achieved high relative density of the sintered monolithic andesite basalt is the result of a carefully performed technological process and accurate determination of the optimal synthesis parameters described in the experimental section. As Fig. 5 evidences, the increase of 316L reduces the relative density of composite materials, which achieves a value of 94.67% in samples containing a maximum amount of 316L, *i.e.*, 30 wt.%. It is expected since it is known that 316L particles present obstacles for fast material transport during sintering and therefore hinder densification of andesite basalt matrix in samples containing large amounts of 316L. Fig. 6 confirms that just few small pores (marked with yellow arrows) were observed on the polished surface of monolithic andesite basalt.

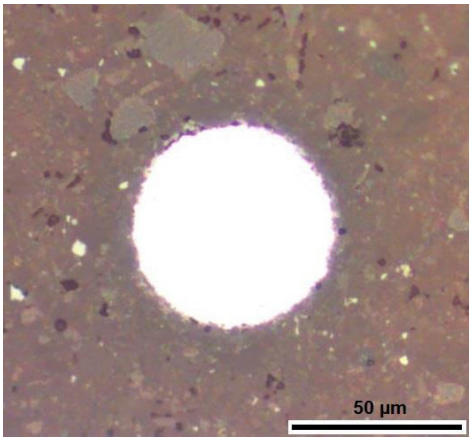

Fig. 7. LOM micrograph of polished surface of the composite material with 20 wt.% of 316L sintered at 1060°C for 60 min.

Fig. 7 shows LOM micrograph of a polished surface of the composite material with 20 wt.% of 316L in the andesite basalt matrix. The 316L grain circular cross-section in the matrix is clearly seen in Fig. 7. The andesite basalt matrix adheres well to the steel grain.

3.2. Shrinkage

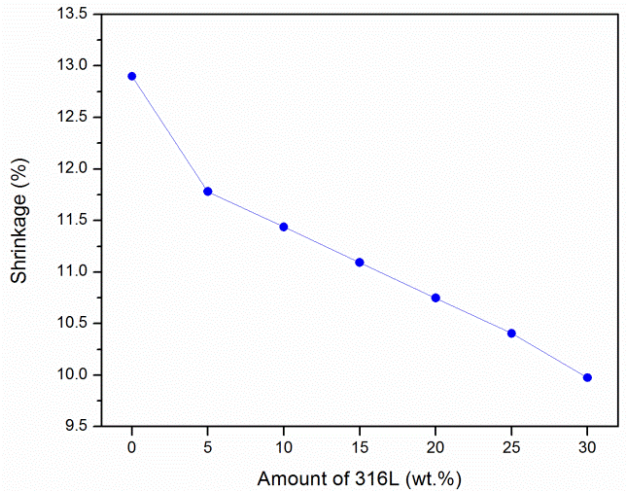

Fig. 8. Effect of 316L amount on shrinkage of the composite samples sintered at 1060°C for 60 min.

The effect of 316L amount on shrinkage of the composite samples after sintering is presented in Fig. 8. which shows that the highest shrinkage of 12.89% was measured in the samples of the monolithic andesite basalt. As the amount of 316L increases, the shrinkage during sintering decreases linearly. The decrease in shrinkage value with an increasing amount of 316L in the composite materials is expected knowing that steel particles do not sinter at 1060°C due to considerably higher sintering temperature. Since the 316L particles do not shrink, the overall shrinkage of the composite is smaller than the monolithic andesite basalt. The minimum shrinkage of 9.97% was measured in the composite material samples containing 30 wt.% of 316L. After sintering, the difference between the minimum and the maximum shrinkage value was 2.92%.

3.3. Weight loss after sintering

The effect of 316L amount on the weight loss of the composite samples after sintering is shown in Fig. 9. From the results presented in Fig. 9, it can be observed that the highest weight loss of 3.43 wt.% was detected for the samples of monolithic andesite basalt. On the other hand, the lowest weight loss of 1.97 wt.% was detected for the samples of composite material with 30 wt.% of 316L. It can be concluded that with the increase of the amount of 316L in the composite materials there is a decrease in weight loss after the sintering, which is expected. During the sintering of monolithic andesite basalt, weight loss occurs due to the hygroscopic moisture evaporation, the chemically bound water removal, burnout of the organic impurities, dissociation of the present carbonates and sulfides, and removal of the gaseous inclusions [49,50] while weight loss of 316L does not occur at the temperature of 1060°C.

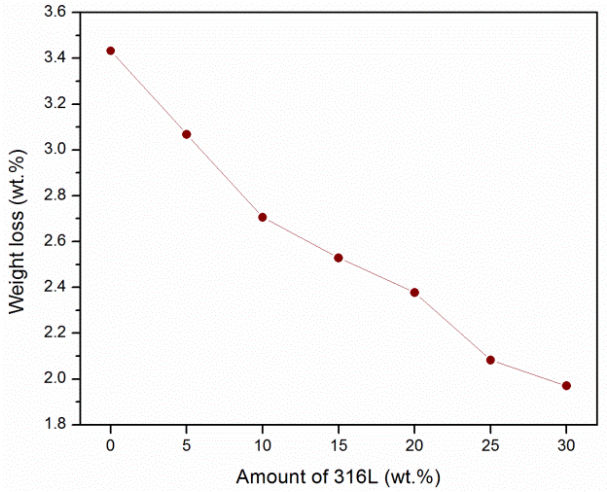

Fig. 9. Effect of 316L amount on weight loss of the composite samples sintered at 1060°C for 60 min.

3.4. Macrohardness

The effect of 316L amount on macrohardness of sintered composites containing 0-30 wt.% of 316L is presented in Fig. 10. The Fig. 10 clearly shows that as the amount of 316L in the samples of composite material increases, the macrohardness of the composite materials decreases. The maximum macrohardness of 6.70±0.05 GPa was measured in the samples of monolithic andesite basalt, while the minimum macrohardness of 6.09±0.24 GPa was measured in the samples of composite material with 30 wt.% of 316L. If compare the values of relative density, shown in Fig. 5, with the values of macrohardness, shown in Fig. 10, it is

clear that with a decrease in relative density there is a decrease in macrohardness of the composite materials, which is expected. Also, the reduction of macrohardness in the composite materials is due to the low hardness of the 316L, which according to the manufacturer's specification is 160 [HV_{30}] [42] *i.e.* 1.569 GPa.

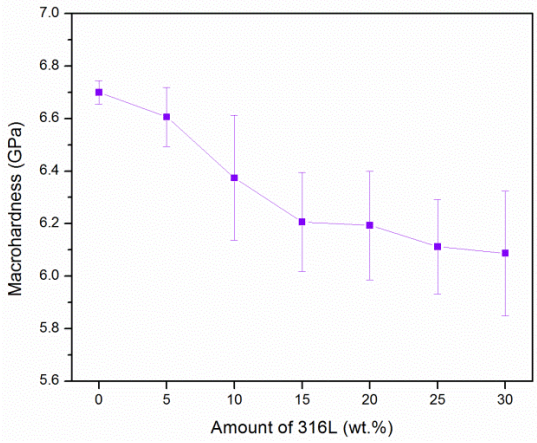

Fig. 10. Effect of 316L amount on macrohardness of the composite samples sintered at 1060°C for 60 min. Variability of the measured macrohardness values is presented with standard deviation.

3.5. Fracture toughness

The effect of 316L amount on fracture toughness of sintered composites containing 0-30 wt.% of 316L is presented in Fig. 11. The presence of the 316L grains in the andesite basalt matrix contributed to the increase of fracture toughness, which is clearly seen in Fig. 11. The minimum fracture toughness of 1.93±0.39 MPa√m was measured in the samples of monolithic andesite basalt. The fracture toughness increases with addition of 316L reaching maximum value of 2.56±0.71 MPa√m in samples containing 20 wt.% of 316L. If compared to the fracture toughness of monolithic andesite basalt it can be concluded that the addition of 20 wt.% of 316L increased fracture toughness of andesite basalt by 32.6%. Further increase of 316L amount above 20 wt.% was followed by the decrease of fracture toughness as a result of low relative density of samples containing above 20 wt.% of 316L (Fig. 5).

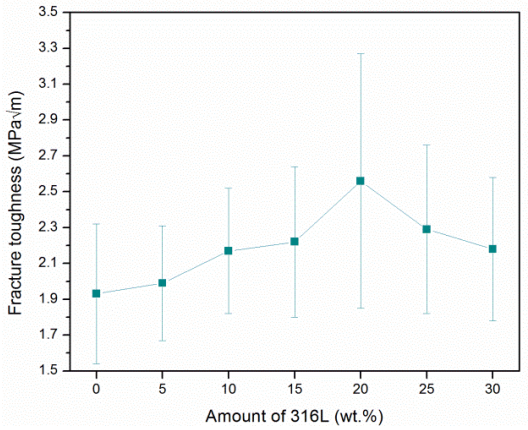

Fig. 11. Effect of 316L amount on fracture toughness of the composite samples sintered at 1060 °C for 60 min. Variability of the measured fracture toughness values is presented with standard deviation.

Fig. 12 shows the indentation mark of the regular four-sided diamond pyramid in the monolithic andesite basalt and four long radial cracks. The cracks are long and radial as the crack tips do not encounter an obstacle (reinforcement) in the monolithic andesite basalt, which can suppress crack propagation and increase the material's fracture toughness.

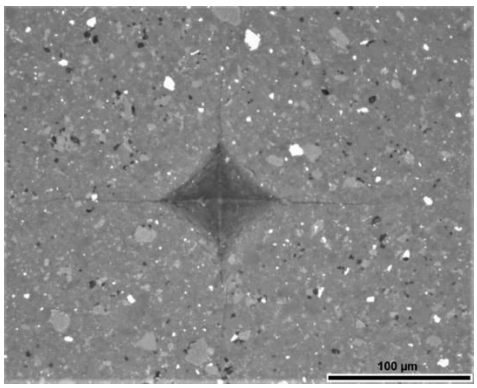

Fig. 12. LOM micrograph showing the indentation mark on the polished surface of monolithic andesite basalt after sintering and four long radial cracks.

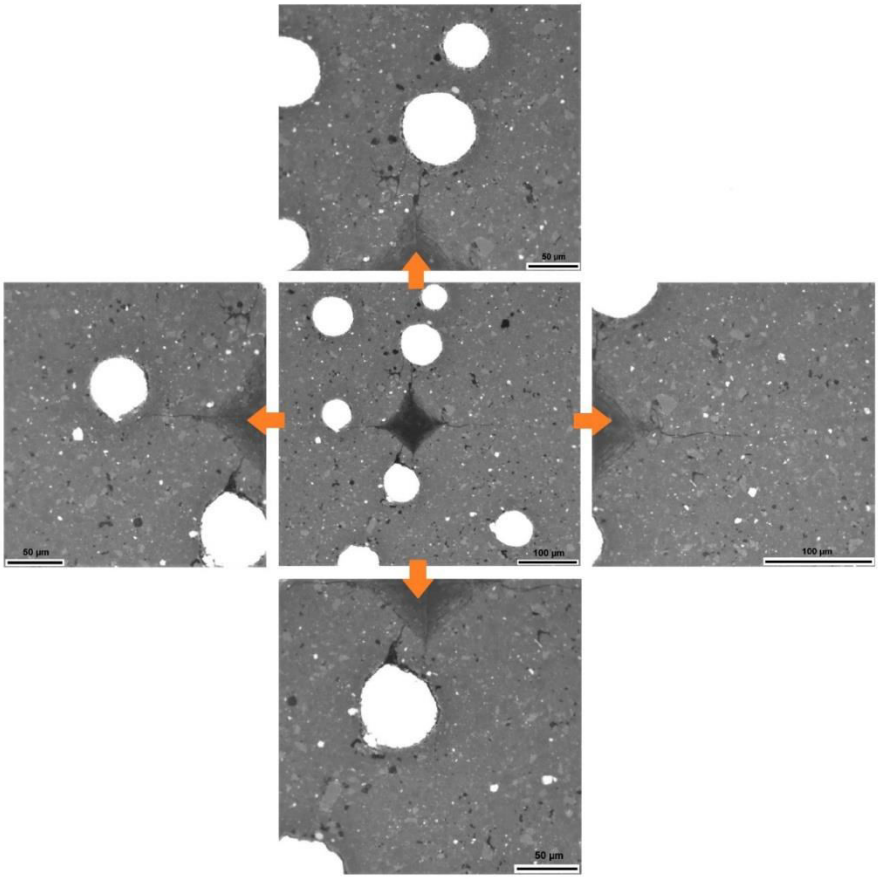

Fig. 13. LOM micrograph show bypasses and stops of the cracks in the andesite basalt matrix when encountering spherical 316L grains in the composite material with 20 wt.% of 316L.

However, as Fig. 13 evidences, the crack length in the sample containing 20 wt.% of 316L is considerably reduced due to the interaction of the crack tip with the steel grains, *i.e.*,

reinforcements, which stop, slow down, and divert crack propagation. This prevents the occurrence of catastrophic failure in the ceramic matrix. Fig. 13 shows the cracks in the andesite basalt matrix and the reinforcement of 316L grains in the composite material with 20 wt.% of 316L. Large grains of the 316L are very effective in activation of the crack deflection toughening mechanism. The crack propagates around the grains losing energy after each deflection due to a decrease of stress concentration at the crack tip [51]. If the extent of debonding is sufficient, the matrix crack bypasses the grain of 316L, leaving it intact. As can be clearly seen in Fig. 13, cracks propagation is no longer radial, as in the monolithic andesite basalt (see Fig. 12). The crack bypasses the reinforcement and thus loses energy, which contributes to increasing the fracture toughness of the composite materials.

Also, an important toughening mechanism that cannot be detected by microscopic observation and is typical for composite materials is toughening due to residual stress created due to the difference in coefficients of thermal expansion of matrix and reinforcing phase. If the reinforcing phase, such as the case in the basalt-stainless steel composite, shrinks more than the matrix during cooling from sintering temperature to room temperature then compressive stress in the matrix, close to the reinforcing phase, will be created [52]. This compressive stress reduces tensile stress at the crack tip, which improves fracture toughness in these composite materials. The formation of compressive residual stress in the composite material also affects cracks' slowdown propagation, thus increasing the fracture toughness. Compressive stress reduces the tensile stress at the crack tip and increases the fracture toughness of the composite materials.

4. Conclusion

Mechanical elements and constructions made of ceramic materials are full of defects that exist even before they are mechanically loaded. Cracks and damage impair the integrity of a structure. Defects, and especially microcracks, constantly grow during exploitation due to the action of external loads, merge with the existing ones until larger cracks appear which can cause a catastrophic fracture. This means that it is very important to prevent the crack from progressing in ceramic materials so as not to jeopardize the integrity of the structure. One of the possible solutions for preventing catastrophic fracture in ceramic material is the production of composite materials with the ceramic matrix and the metal reinforcement which is presented in this paper.

Based on the obtained experimental results, the following can be concluded:

- Applying the technological process, which consists of: milling, homogenization, pressing and sintering in air, the basalt-stainless steel composite materials can be obtained, using andesite basalt and 316L austenitic stainless steel as starting materials.
- As the amount of 316L increases, the relative density of the composite materials decreases. The highest relative density of 99.81% was measured in the monolithic andesite basalt.
- As the amount of 316L increases, the shrinkage of the composite materials decreases. The highest shrinkage of 12.89% was measured in the monolithic andesite basalt.
- As the amount of 316L increases, the weight loss of the composite materials decreases. The minimum weight loss of 1.97 wt.% was measured in the composite material with 30 wt.% of 316L.
- As the amount of 316L increases, the macrohardness of the composites decreases as a function of relative density. The highest macrohardness of 6.70±0.05 GPa was measured in the monolithic andesite basalt.

- As the amount of 316L increases up to 20 wt.%, the fracture toughness increases and reach the maximum of 2.56±0.71MPa√m in the composite material with 20 wt.% of 316L, which is 32.6% higher than the monolithic andesite basalt which value is 1.93±0.39 MPa√m.

Key reasons why a crack bypasses or stops in front of the 316L grains, which contributes to the increased fracture toughness of the composite materials:

- The 316L grains are ductile as opposed to brittle andesite basalt grains, so the crack spreads more easily through the brittle than through the ductile zone.
- The 316L steel grains are spherical, which causes the crack to lose energy when it bypasses them.
- The boundary between the matrix and the reinforcements is the weakest part of the composite material. For this reason, a crack propagates around the 316L grain and so loses energy. Bearing in mind that the crack always moves along the line of the smaller resistance.
- The creation of residual compressive stress around the 316L grains, due to different coefficients of thermal expansion of the matrix and reinforcements, stops or redirects the propagation of the crack.

Composite materials are rightly considered materials that will represent the main direction of innovation in the near and distant future of novel materials.

Acknowledgments

This work was financially supported by the Ministry of Education, Science, and Technological Development of the Republic of Serbia (Contract No. 451-03-9/2021-14/200017). Authors would like to acknowledge the help of Dr. Smilja Marković from the Institute of Technical Sciences of The Serbian Academy of Sciences and Arts (SASA), Serbia, during the particle size distribution analysis.

5. References

1. J. S. Reed, Principles of Ceramics Processing, John Wiley & Sons, Inc., New Yirk, 1995.
2. M. W. Barsoum, Fundamentals of Ceramics, McGraw-Hill, 2003.
3. W. D. Callister, D. G. Rethwisch, Materials Science and Engineering: An Introduction, John Wiley & Sons, Inc., 8th ed, 2010.
4. G. D. Quinn, Fractography of Ceramics and Glasses, National Institute of Standards and Technology, 2nd ed, 2016.
5. D. W. Kingery, H. K. Bowen, D. R. Uhlmann, Introduction to Ceramics, John Wiley & Sons, New York, 1976.
6. R. W. Davidge, Mechanical Behaviour of Ceramics, Cambridge University Press, Cambridge, 1979.
7. J. B. Wachtman, Mechanical Properties of Ceramics, Wiley-Interscience, New York, Chichester, 1996.
8. D. Munz, T. Fett, Ceramics, Springer, Berlin, Heidelberg, 1999.
9. D. Broek, The Practical Use of Fracture Mechanics, Kluwer Academic Publishers, London, 1989.
10. R. Danzer, T. Lube, P. Supancic, R. Damani, Adv. Eng. Mater., 10 (4) (2008) 275.
11. G. Gupta, A. Kumar, R. Tyagi, S. Kumar, Int. J. Innov., 5 (5) (2016) 6907.

12. S. A. Morse, Basalts and Phase Diagrams: An Introduction to the Quantitative Use of Phase Diagrams in Igneous Petrology, Springer-Verlag, New York (US), 1980.
13. A. I. Poznyak, I. A. Levitskii, S. E. Barantseva, Glas. Ceram., 69 (7-8) (2012) 262.
14. S. Kapur, N. Sakarya, C. Karaman, E. A. Fitzpatrick, M. Pagliai, Brit. Ceram. Trans., 94 (1) (1995) 33.
15. M. Kirsch, G. Berger, U. Banach, T. Hubert, Intercer., 37 (3) (1988) 34.
16. B. Matović, S. Bošković, M. Logar, J. Serb. Chem. Soc., 68 (6) (2003) 505.
17. A. Todić, D. Čikara, T. Todić, B. Ćirković, IMK 14 R&D, 15 (3-4) (2009) 25. (in Serbian)
18. G. A. Khater, M. O. Abu Safiah, E. M. A. Hamzawy, Process. Appl. Ceram., 9 (2) (2015) 117.
19. S. Matkó, S. Keszei, I. Csontos, P. Anna, G. Marosi, M. Zsuga, J. Borda, G. Nagy, Macromol. Symp., 233 (2006) 217.
20. M. C. Wang, Z. G. Zhang, Y. B. Li, J. Reinf. Plast. Comp., 27 (4) (2008) 393.
21. A. Prstić, R. Simić, Lj. Andrić, Z. Aćimović, in: "X Balkan Mineral Processing Congress: Mineral Processing in 21st Century", Varna, 2003, p. 893-897.
22. A. Prstić, Z. Aćimović-Pavlović, Lj. Andrić, M. Ćosić, Z. Aćimović, in: "XI Balkan Mineral Processing Congress: Mineral Processing in Sustainable Development", Tirana, 2005, p. 422-425.
23. G. H. Beall, H. L. Rittler, Am. Ceram. Soc. Bull., 55 (6) (1976) 579.
24. [24] M. Pavlović, M. Sarvan, F. Klisura, Z. Aćimović, in: "4th Conference Maintenace", Zenica, 2016, p. 175-183.
25. [25] M. Pavlović, M. Đuričić, A. Mumđić, in: "Conference SED", Užice, 2015, p. 53-60.
26. D. Čikara, A. Todić, D. Čikara-Anić, FME Trans., 38 (4) (2010) 203.
27. Lj. Andrić, Z. Aćimović-Pavlović, M. Trumić, A. Prstić, Z. Tanasković, Mater. Des., 39 (2012) 9.
28. D. Čikara, A. Todić, T. Todić, IMK 14 R&D., 16 (37) (2010) 1. (in Serbian)
29. B. Wei, H. Cao, S. Song, Mat. Sci. Eng. A. – Struct., 527 (18-19) (2010) 4708.
30. J. Maletaškić, B. Todorović, M. Gilić, M. Marinović Cincović, K. Yoshida, A. Gubarevich, B. Matović, Sci. Sinter., 52 (2020) 41.
31. F. AbuSahmin, A. Algellai, N. Tomić, M. M. Vuksanović, J. Majstorović, T. Volkov Husović, V. Simić, R. Jančić Heinemann, M. Toljić, J. Kovačević, Sci. Sinter., 52 (2020) 67.
32. L. Abosrra, A. F. Ashour, S. C. Mitchell, M. Zouseffi, WIT Trans. Eng. Sci., 65 (12) (2009) 161.
33. C. Xu, Y. Zhang, G. Cheng, W. Zhu, Chinese J. Chem. Eng., 14 (6) (2006) 829.
34. J. Xu, C. Zhuo, J. Tao, S. Jiang, L. Liu, J. Phys. D: Appl. Phys., 42 (2009) 015410.
35. T. Mathiesen, J. Rau, J. E. Frantsen, J. Terävä, P-Å. Björnstedt, B. Henkel, Pharm. Eng., 21 (4) (2002).
36. N. Kurgan, Y. Sun, B. Cicek, H. Ahlatci, Cninese Sci. Bull., 57 (15) (2012) 1873.
37. M. D. Mihailović, A. S. Patarić, Z. P. Gulišija, Z. V. Janjušević, M. D. Sokić, Hem. Ind., 67 (5) (2013) 753. (in Serbian)
38. B. G. Pound, Corros. Rev., 32 (1-2) (2014) 21.
39. J. H. Reinshagen, A. J. Neupaver, in: "Advances in Powder Metallurgy", Princeton, N.J.: Metal Powder Industries, 1989, p. 283-295.
40. A. U. Malik, P. C. Mayan Kutty, N. A. Siddiqi, I. N. Andijani, S. Ahmed, Corros. Sci., 33 (11) (1992) 1809.
41. E. Albert, M. Muntean, A. Ianculescu, F. Miculescu, B. Albert, Adv. Mat. Res., 59 (2009) 39.
42. Surfit™ 316L Product Data Sheet – Serfla. http://www.serfla.com.br/pdf/316L.pdf
43. D. Božić, M. Vilotijević, J. Ružić, U. Jovanović, J. Stašić, Sci. Sinter., 48 (2016) 293.

44. N. P. Karapatis, G. Egger, P. E. Gygax, R. Glardon, in: "Proceedings of the 9th Solid Freeform Fabrication Symposium", Austin (USA), 1999, p. 255-263.
45. B. Matovic, J. Maletaskic, J. Zagorac, V. Pavkov, R. S. S. Maki, K. Yoshida, T. Yano, J. Eur. Ceram. Soc., 40 (7) (2020) 2652.
46. V. Pavkov, G. Bakić, V. Maksimović, I. Cvijović-Alagić, M. Prekaski Đorđević, D. Bučevac, B. Matović, Process. Appl. Ceram., (2022) (in Press).
47. A. G. Evans, E. A. Charles, J. Am. Ceram. Soc., 59 (7-8) (1976) 371.
48. T. Do, T. J. Bauder, H. Suen, K. Rego, J. Yeom, P. Kwon, in: "13th International Manufacturing Science and Engineering Conference", College Station, TX, 2018, p. 1-10.
49. S. V. Fomichev, N. P. Dergacheva, A. V. Steblevskii, V. A. Krenev, Theor. Found. Chem. Eng., 45 (4) (2011) 526.
50. N. F. Drobot, O. A. Noskova, A. V. Khoroshilov, A. V. Steblevskii, S. V. Fomichev, V. A. Krenev, Inorg. Mater., 50 (3) (2014) 314.
51. K. T. Faber, A. G. Evans, Acta. metall., 31 (4) (1983) 565.
52. Z. Ling, Y. L. Wu, J. Mater. Sci., 42 (2007) 759.

Сажетак: *У овом раду је приказан технолошки процес добијања композитних материјала базалт-нерђајући челик, као и испитивање њихових физичких и механичких својстава. Технолошки процес се састоји од следећих фаза: млевење, хомогенизација, пресовање и синтеровање у циљу добијања композитних материјала са побољшаном жилавошћу лома. Као матрица у композитним материјалима коришћен је андезит базалт са локалитета „Доње Јариње", Србија, док је као ојачавач коришћен комерцијални аустенитни нерђајући челик 316L у садржају 0-30 теж.%. Иако је повећање садржаја 316L изазвало континуално смањење релативне густине синтерованих узорака, релативна густина узорака који садрже 30 теж.% 316L била је изнад 94%. Зрна 316L, која поседују већи коефицијент топлотног ширења од базалтне матрице, брже се скупљају током хлађења након синтеровања, што доводи до стварања притисних заосталих напона у базалтној матрици која окружује сферна зрна челика. Присуство заосталог напрезања створило је услове за активирање механизама ојачавања као што су скретање прслине и ојачавање услед притисних заосталих напона. Додавање 20 теж.% честица 316L као ојачавача повећало је жилавост лома базалта за више од 30%. Измерена вредност релативне густине ових узорака је 97%, док је вредност макротврдоће 6,2 GPa.*

Кључне речи*: композитни материјали, андезит базалт, нерђајући челик 316L, синтеровање, прслине.*